SUPPLEMENTAL MATERIAL

SUPPLEMENTAL METHODS

Animals. Generation of RyR2-S2814A knock-in and AC3I transgenic mice was described previously [1, 2]. RyR2-S2814D knock-in mice were created using a similar approach described for RyR2-S2814A knock-in mice [1]. Briefly, a genomic clone containing exons 56 and 57 of the mouse *Ryr2* gene was cloned into a pDTA4B vector using homologous recombination. The S2814D mutation was introduced along with a silent ClaI restriction site into exon 56 of *Ryr2* by site-directed mutagenesis. The final targeting vector was obtained by cloning a lox P-flanked Neo cassette into intron 56 of *Ryr2*. After linearization with PmeI, the targeting vector was electroporated into AB2.2 129Sv/J ES cells. Successfully targeted ES cell clones were identified by Southern blot and injected into blastocysts to generate chimeric mice. Germline transmission was verified by PCR analysis and positive offspring was crossed with Meox2-Cre mice to allow genetic excision of the Neo cassette. Heterozygous RyR2-S2814D mice were mated to obtain RyR2-S2814D homozygous knock-in mice and WT littermates. The RyR2-S2814A and RyR2-S2814D knock-in mice, and AC3-I transgenic mice, have all been backcrossed into C57Bl/6 mice for 7-10 generations. Homozygous RyR2-S2814A and RyR2-S2814D knock-in mice were littermates of the WT mice. Numbers of mice studied includes: WT (n = 89), S2814D (n = 66), S2814D x AC3I (n = 24), and S2814A (n = 16). All animal studies were performed according to protocols approved by the Institutional Animal Care and Use Committee of Baylor College of Medicine conforming the *Guide for the Care and Use of Laboratory Animals* published by the U.S. National Institutes of Health (NIH Publication No. 85-23, revised 1996).

Co-Immunoprecipitation Assay. RyR2 was immunoprecipitated from heart lysates using an anti-RyR2 antibody (Thermo Scientific, Rockland, IL) incubated with Protein A-Sepharose beads

(Rockland, Gilbertsville, PA) at room temperature for 1 h. For co-immunoprecipitation, antibody-attached beads were incubated with heart lysate aliquots containing 1000 μg total protein at 4ºC overnight. The 1 mL reaction consisted of Co-IP buffer containing 50 mM Tris-Cl, pH 7.4, 150 mM NaCl, 1% CHAPS, 20 mM NaF, 1 mM Na_3VO_4, 1x protease inhibitors and 1x phosphatase inhibitors (Roche, Basel, Switzerland) and 0.3% Triton x-100. Post-incubation, beads were washed with detergent-free Co-IP buffer, and resuspended in 2x LDS buffer (Invitrogen, Carlsbad, CA) containing β-mercaptoethanol. Samples were heated at 50ºC for 15 min, and were resolved on 4-20% Criterion SDS-PAGE gels (Bio-Rad) for detection of RyR2 and FKBP12.6. Western blotting on resolved gels was performed as described below using monoclonal anti-RyR2 antibody and polyclonal anti-FKBP12.6 antibody (Thermo Fisher).

Western blot analyses. Heart lysates were prepared from flash-frozen mouse hearts as described previously [3]. Lysates were taken from mice at rest (Fig. 1), post-TAC or post-sham surgery (Fig. 7 and S5), immediately after pacing (Fig. 5 and S4), and with/without exposure to pacing (Fig. 7). Heart lysate aliquots were size-fractionated on 6% (for RyR2) or 12% (for Cav1.2, NCX1, SERCA2a, CaMKII, and GAPDH) or 15% (for PLN) SDS-polyacrylamide gels. For PLN-monomer blots, heart lysates were heated at 70 °C for 10 min in 1x sample loading buffer containing 5% β-mercaptoethanol before loading on gels. The resolved gels were electro-transferred on PVDF membranes. The membranes were probed with anti-pSer2808-RyR2 (1:1,000), anti-pSer2814-RyR2 (1:500) (both custom-made for our lab [1, 3]), anti-pSer16-PLN (1:5,000), anti-pThr17-PLN (1:2,500) (latter two from Badrilla Ltd., Leeds, United Kingdom), anti-CaMKIIδ (1:200), anti-Cav1.2 (1:200; Alomone Labs, Jerusalem), anti-NCX1 (1:500; Swant, Bellinzona, Switzerland), anti-SERCA2a (1:500; Santa Cruz Biotechnology, Santa Cruz, CA) polyclonal antibody, anti-RyR2 (1:5,000), anti-PLN (1:1000) (both Thermo Fisher Scientific (Pierce), Rockford, IL), or anti-GAPDH (1:5,000; Millipore, Temecula, CA) monoclonal antibody

at 4°C either overnight or at room temperature for 4 h. They were developed using Alexa-Fluor680-conjugated anti-mouse (Invitrogen Molecular Probes, Carlsbad, CA) and/or IR800Dye-conjugated anti-rabbit fluorescent secondary antibodies (Rockland Immunochemicals, Gilbertsville, PA), and scanned on an Odyssey infrared scanner (Li-Cor, Lincoln, NE). Integrated densities of protein bands were measured using ImageJ Data Acquisition Software (National Institute of Health, Bethesda, MD). Protein-signal densities were normalized to the corresponding GAPDH-signal densities, while phosphorylation-signal densities were normalized to the corresponding total protein-signal densities, and used for plotting data. Student T-tests were used to compare data in two sample groups.

Confocal imaging. Ca^{2+} sparks were recorded in saponin-permeabilized (50 μg/ml) or intact ventricular cardiomyocytes. Permeabilized cells were placed in an internal solution (in mM): EGTA 0.5; HEPES 10; K-aspartate 120; MgATP 5; free $MgCl_2$ 1; reduced glutathione 10; free [Ca^{2+}] 50nM; creatine phosphokinase 5U/ml; phosphocreatine 10; dextran (MW: 40,000) 4%; fluo-4 K-salt 0.025; pH 7.2). PKA activity was prevented by using PKA inhibitory peptide PKI (15 μmol/L). Endogenous CaMKII activation was obtained by elevated [Ca^{2+}] (500 nM), exogenous calmodulin (1.2 μM) and okadaic acid (2 μM) as previously described [4]. After incubation with endogenous CaMKII activation solution for 1 minute, myocytes were superfused with original internal solution containing 10 μM okadaic acid to wash off phosphorylating solution and preserve phosphorylation while Ca^{2+} sparks were recorded again. CaMKII activity was inhibited by AIP administration (1 μM). Intact ventricular myocytes were loaded with Fluo-3 AM (5 μM, Molecular Probes) and Ca^{2+} transients were recorded as previously described [5]. Ca^{2+} transients were obtained by field stimulation at 1 Hz in normal Tyrode's solution (in mM): 140 NaCl, 4 KCl, 1.1 $MgCl_2$, 10 HEPES, 10 glucose, 1.8 $CaCl_2$; pH7.4 with NaOH. SR Ca^{2+} load was evaluated by Ca^{2+} transient upon rapid caffeine application (10 mM). Experiments were performed on confocal microscopy (BioRad, Radiance 2100, 40x objective) using line scan mode with argon

laser (λ_{ex} 488 nm, λ_{em} >505 nm). Image analysis used ImageJ software and homemade routines in IDL (interactive data language).

Single channel recordings. The *trans* chamber (1.0 ml of 250 mM HEPES and 53 mM $Ca(OH)_2$, 50 mM KCl, pH 7.35) representing the intra-SR compartment was connected to the head stage input of a bilayer voltage-clamp amplifier. The *cis* chamber (1.0 ml of 250 mM HEPES, 125 mM Tris, 50 mM KCl, 1.0 mM EGTA, and 0.5 mM $CaCl_2$, pH 7.35) representing the cytoplasmic compartment was held at virtual ground. Free [Ca^{2+}] was calculated by CHELATOR software. At the conclusion of each experiment, ryanodine (5 μmol/L) or ruthenium red (20 μmol/L) was applied to confirm RyR2 channel identity.

ECG telemetry. Transmitters (Data Sciences International, St. Paul, MN) were implanted in the abdominal cavity with subcutaneous electrodes in lead II configuration. Telemetry was recorded > 48 h after surgery in ambulatory, unanesthetized mice for 24 hours total for baseline measurements. Interventional analysis was performed at baseline and also after intraperitoneal (i.p.) injection of 100 μg isoproterenol (Sigma Aldrich, St. Louis). Additionally, on a separate day, ECG's were recorded before and after caffeine and epinephrine (120 mg/kg and 2 mg/kg, respectively, Sigma Aldrich) injection i.p. Data collection, which started 1 hour before the intervention and continued for 2-3 hours after injection, was performed using Dataquest software. Off-line data analyses was performed by using ECG Auto analysis software, version 4.1 (Data Sciences International).

Programmed electrical stimulation. Mice were anesthetized using 1.5 % isofluorane in 95% O_2. ECG channels were amplified (0.1 mV/cm) and filtered between 0.05 and 400 Hz). A computer-based data acquisition system (Emka Technologies) was used to record a 6-lead body surface ECG, and up to 4 intracardiac bipolar electrograms. Bipolar right atrial pacing and

right ventricular pacing was performed using 2-ms current pulses delivered by an external stimulator (STG-3008, MultiChannel Systems, Reutlingen, Germany). Standard clinical electrophysiologic pacing protocols were used to determine all basic electrophysiologic parameters. Ventricular effective refractory period was determined at three drive cycle lengths. Overdrive pacing and single, double, and triple extrastimuli were delivered to determine inducibility of VT, which were tested twice. After baseline measurements were completed, and VT inducibility was tested via pacing, isoproterenol (0.5 mg/kg, Sigma Aldrich, St. Louis) or propranolol (3 mg/kg, Sigma Aldrich, St. Louis) were administered, and pacing protocols were repeated to assess the effects on conduction and refractoriness.

Transverse aortic constriction. Mice were anesthetized using a mixture of 2% isoflurane and 95% O_2. TAC was created by subjecting the aorta to a defined, 27-gauge constriction using a 6-0 suture between the first and second truncus of the aortic arch. A computer-based Doppler signal processor (Indus Instruments, Houston, TX) was used to measure Doppler velocities in the right and left carotid arteries. Right/left carotid peak velocity ratios were similar in S2814A and WT littermates, or S2814D and WT littermates, respectively.

SUPPLEMENTAL TABLES

Table S1.

ANOVA Evaluation of Echocardiographic Parameters

Age	ANOVA Statistics			
	df	Mean Square	F	*p*
HR (bpm)	3	3450.4	1.8	0.2
EF (%)	3	114.4	4.8	0.005
FS (%)	3	44.8	4.5	0.007
ESD (mm)	3	0.5	6.2	0.001
EDD (mm)	3	0.4	5.2	0.003
IVSs (mm)	3	0.01	1.5	0.2
IVSd (mm)	3	0.03	3.0	0.04
LVPWs(mm)	3	0.07	3.1	0.04
LVPWd(mm)	3	0.09	4.6	0.006

HR = heart rate; bpm = beats per minute; EF = ejection fraction; FS = left ventricular fractional shortening; ESD = end-systolic diameter; EDD = end-diastolic diameter; IVSs/ IVSd = intraventricular septal wall thickness in systole/ diastole; LVPWs/ LVPWd = left ventricular posterior wall thickness in systole/diastole. 2-way ANOVA was used to compare groups. Degrees of freedom (df), mean square, the F statistic, and *p* values are displayed in the ANOVA statistics heading.

Table S2.

Electrophysiological intervals recorded using ECG telemetry in WT, S2814D and S2814D:AC3I mice.

	WT (n = 10)	S2814D (n = 13)	S2814D:AC3I (n = 11)
RR (ms)	91.6 ± 2.1	97.5 ± 4.4	99.5 ± 5.0
PQ (ms)	27.5 ± 0.9	28.4 ± 1.1	32.7 ± 1.7 *
QRS (ms)	8.9 ± 0.5	9.2 ± 0.4	10.1 ± 0.2 *
QT (ms)	35.1 ± 1.4	32.5 ± 1.5	38.3 ± 1.0 *
QTc (ms)	60.0 ± 1.4	55.5 ± 1.9	60.7 ± 2.0
SCL (ms)	92.3 ± 2.3	97.2 ± 4.6	98.6 ± 5.4
AV (ms)	33.9 ± 0.9	35.0 ± 0.9	38.7 ± 2.0

Data are expressed as mean ± SEM. RR, time interval between two consecutive RR waves; PQ, interval from the beginning of the P wave to the peak of the Q wave; QRS, duration of the interval between begining of Q wave to peak of S wave; QT, interval from beginning of Q wave to the end of the T wave; QTc, QT interval corrected for heart rate; SCL, sinus cycle length time; AV, interval from the beginning of the P wave to the beginning of the QRS complex. *P<0.05 versus WT.

Table S3.

Electrophysiological intervals in WT and S2814D mice.

	WT (n = 8)	S2814D (n = 9)	S2814D:AC3I (n = 12)
AERP (ms)	31.1 ± 3.3	30.7 ± 0.7	32.5 ± 1.7
VERP (ms)	26.2 ± 1.5	24.1 ± 2.3	24.6 ± 0.7

Data are expressed as mean ± SEM. AERP, atrial effective refractory period; VERP, ventricular effective refractory period. *P<0.05 versus WT.

Table S4.

Echocardiographic parameters of WT and S2814A mice 8 weeks post-TAC surgery

	8 Weeks Post-TAC	
	WT (n = 14)	**S2814A (n = 13)**
HR (bpm)	475.1 ± 22.0	474.3 ± 13.71
EF (%)	36.6 ± 6.1	34.2 ± 4.4
FS (%)	17.8 ± 3.2	16.6 ± 2.3
ESD (mm)	3.69 ± 0.37	3.76 ± 0.3
EDD (mm)	4.45 ± 0.29	4.45 ± 0.25
IVSs (mm)	0.87 ± 0.02	0.84 ± 0.02
IVSd (mm)	0.78 ± 0.01	0.75 ± 0.02
LVPWs	1.06 ± 0.05	1.05 ± 0.05
LVPWd (mm)	0.83 ± 0.03	0.89 ± 0.03

Data are expressed as mean ± SEM. HR = heart rate; bpm = beats per minute; EF = ejection fraction; FS = left ventricular fractional shortening; ESD = end-systolic diameter; EDD = end-diastolic diameter; IVSs/IVSd = inraventricular septal wall thickness in systole/diastole; LVPWs/ LVPWd = left ventricular posterior wall thickness in systole/diastole. *$P < 0.05$ versus WT.

SUPPLEMENTAL FIGURE LEGENDS

Figure S1. Generation of RyR2-S2814D knockin mice. (**A-E**) Schematic overview of gene targeting strategy. A genomic clone harboring exon 56 and 57 of *Ryr2* was isolated from a BAC (**A**) and subcloned using homologous recombination (**B**). The nucleotide sequence coding for the S to D mutation was introduced along with a silent ClaI site and a lox P-flanked Neo-cassette (**C**) to obtain the final targeting vector. This targeting vector was electroporated into ES cells for genomic recombination (**D**). Positive ES cells were injected into blastocysts to generate chimeric mice. Positive offspring was crossed with Meox2-Cre mice to establish excision of the Neo cassette (**E**). (**F**) Successful recombination in ES cells was verified by Southern blot after digesting DNA with EcoRV. (**G**) Heterozygous mice were mated to obtain homozygous RyR2-S2814D mice and WT littermates as determined by PCR on tail digests and subsequent ClaI digestion.

Figure S2. **Calcium spark characteristics for permeabilized cardiomyocytes.** (**A**) Calcium spark amplitude in permeabilized myocytes in the absence (-) or presence (+) of CaMKII. There were no differences between the genotypes. (**B**) Calcium spark full duration at half-maximum (FDHM) was not different among WT, S2814D, and S2814A myocytes, with or without activation of endogenous CaMKII. (**C**) Full width at half-maximum (FWHM) was not different among WT, S2814D, and S2814A permeabilized myocytes in the presence or absence of CaMKII. (**D**) Maximum release of SR Ca^{2+} was not different in WT, S2814D, and S2814A permeabilized myocytes in the presence or absence of CaMKII. N is shown in bar graphs.

Figure S3. **Increased calcium spark frequency in intact cardiomyocytes from S2814D mice.** (**A**) Ca^{2+} spark frequency (CaSpF) in WT, S2814D, and S2814A intact cardiomyocytes, showing that myocytes from S2814D mice exhibited a significantly increased CaSpF. (**B**) Ratio

of CaSpF to SR Ca^{2+} load. S2814D intact myocytes had a significantly higher ratio compared to WT myocytes. (**C**) Mean Ca^{2+} spark amplitude in WT, S2814D, and S2814A intact myocytes were not different. (**D**) Ca^{2+} spark full duration at half-maximum (FDHM) was not different in WT, S2814D, and S2814A intact myocytes. (**E**) Full width at half-maximum (FWHM) was not different among WT, S2814D, and S2814A intact myocytes. (**F**) Ca^{2+} transient time to peak measured in seconds. There were no differences among WT, S2814D, and S2814A intact myocytes. Values are expressed as mean ± SEM. N is shown in bar graphs. **P*<0.05, ***P*<0.01.

Figure S4. Intracardiac pacing does not alter phosphorylation of PKA targets. (**A**) Representative Western blot of the RyR2 PKA site (S2808) in WT and S2814D mice before and after intracardiac pacing. (**B**) Bar graph showing that pacing did not change PKA phosphorylation of RyR2. (**C**) Representative Western blot of the phospholamban (PLN) PKA site (S16). (**D**) Bar graph showing that pacing did not change PKA phosphorylation of PLN. N is shown in bar graphs.

Figure S5. TAC surgery does not increase RyR2 phosphorylation at 4 weeks. (**A**) Representative Western blots showing total RyR2 and CaMKII-phosphorylated RyR2 at 2814 in WT and S2814D mice at 4 weeks after transverse aortic constriction (TAC). (**B**) Bar graphs showing averaged ratio between phosphorylated RyR2-pS2814 and total RyR2. At four weeks post-TAC, WT mice showed a trend towards increased phosphorylation only; CaMKII phosphorylation of RyR2 was prevented in S2814D mice. (**C**) Representative Western blots showing total RyR2 and PKA-phosphorylated RyR2 at S2808 in WT and S2814D mice at 4 weeks after TAC. (**D**) Bar graphs showing averaged ratio between phosphorylated RyR2-pS2808 and total RyR2. There were no significant differences between the groups at the PKA site. N is shown in bar graphs. *P<0.05 versus surgically matched controls.

Figure S1

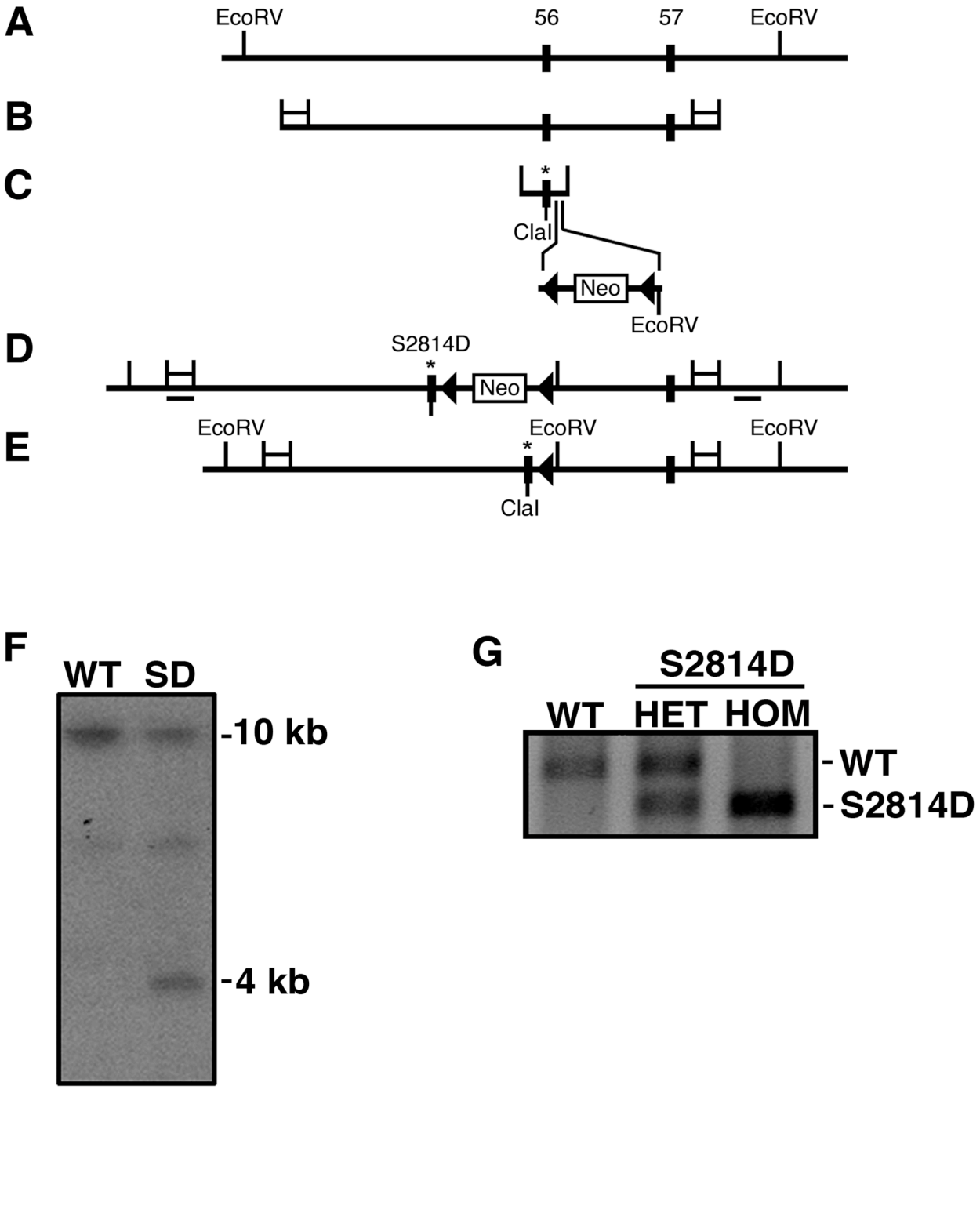
A
EcoRV
56
57
EcoRV
B
C
ClaI
Neo
EcoRV
D
S2814D
Neo
E
EcoRV
EcoRV
EcoRV
ClaI
F
WT SD
-10 kb
-4 kb
G
S2814D
WT HET HOM
-WT
-S2814D

Figure S2

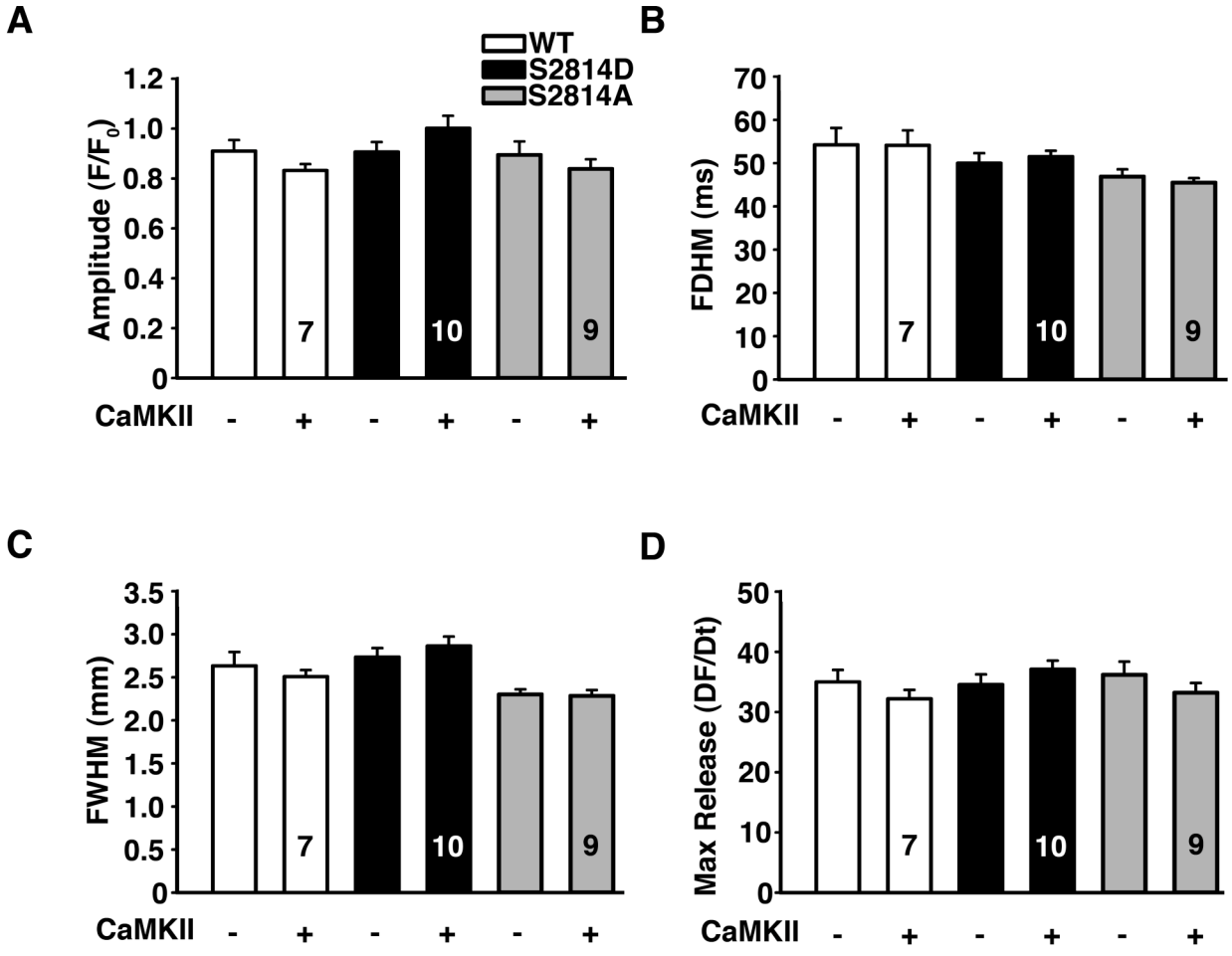
A
WT
S2814D
S2814A
Amplitude (F/F0)
1.2
1.0
0.8
0.6
0.4
0.2
0
7
10
9
CaMKII - + - + - +
B
FDHM (ms)
70
60
50
40
30
20
10
0
7
10
9
CaMKII - + - + - +
C
FWHM (mm)
3.5
3.0
2.5
2.0
1.5
1.0
0.5
0
7
10
9
CaMKII - + - + - +
D
Max Release (DF/Dt)
50
40
30
20
10
0
7
10
9
CaMKII - + - + - +

Figure S3

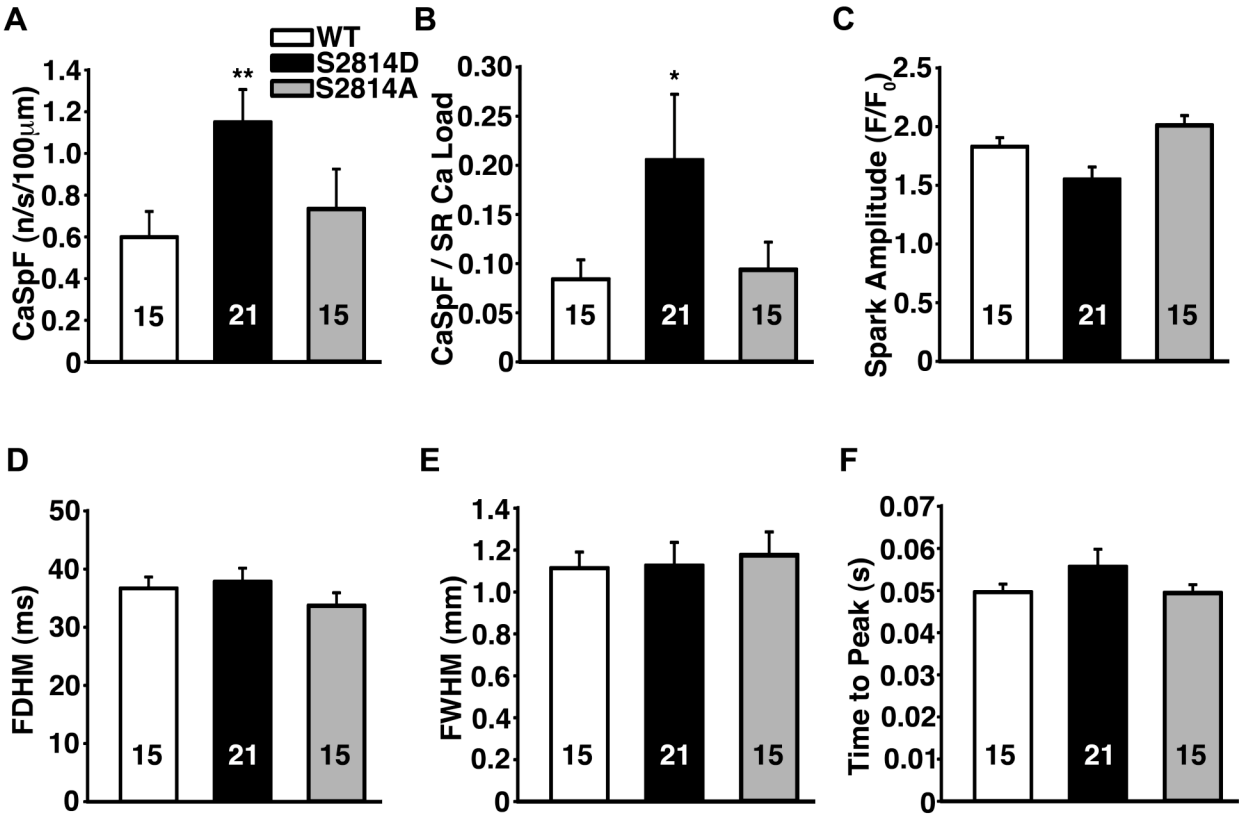
A
WT
S2814D
S2814A
CaSpF (n/s/100μm)
1.4
1.2
1.0
0.8
0.6
0.4
0.2
0
**
15
21
15
B
CaSpF / SR Ca Load
0.30
0.25
0.20
0.15
0.10
0.05
0
*
15
21
15
C
Spark Amplitude (F/F0)
2.5
2.0
1.5
1.0
0.5
0
15
21
15
D
FDHM (ms)
50
40
30
20
10
0
15
21
15
E
FWHM (mm)
1.4
1.2
1.0
0.8
0.6
0.4
0.2
0
15
21
15
F
Time to Peak (s)
0.07
0.06
0.05
0.04
0.03
0.02
0.01
0
15
21
15

Figure S4

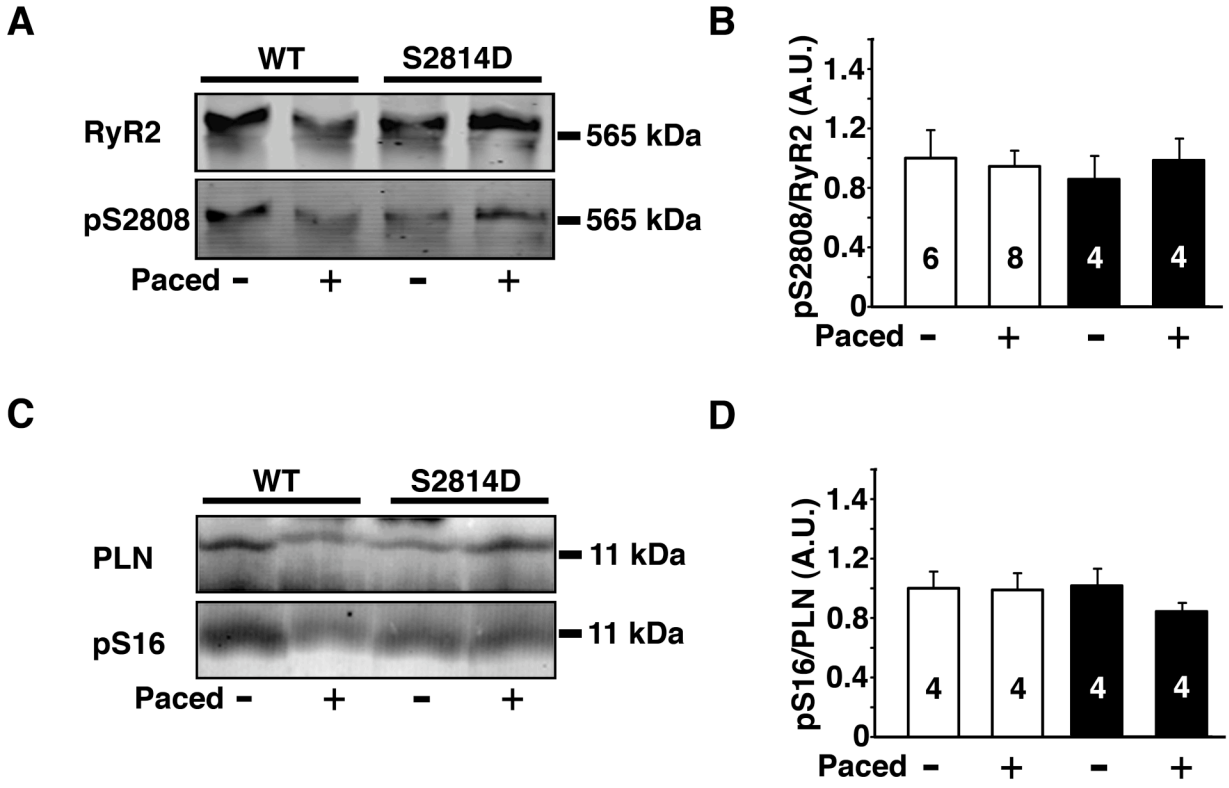
A
WT
S2814D
RyR2
565 kDa
pS2808
565 kDa
Paced - + - +
B
pS2808/RyR2 (A.U.)
1.4
1.2
0.8
0.4
0
6
8
4
4
Paced - + - +
C
WT
S2814D
PLN
11 kDa
pS16
11 kDa
Paced - + - +
D
pS16/PLN (A.U.)
1.4
1.2
0.8
0.4
0
4
4
4
4
Paced - + - +

Figure S5

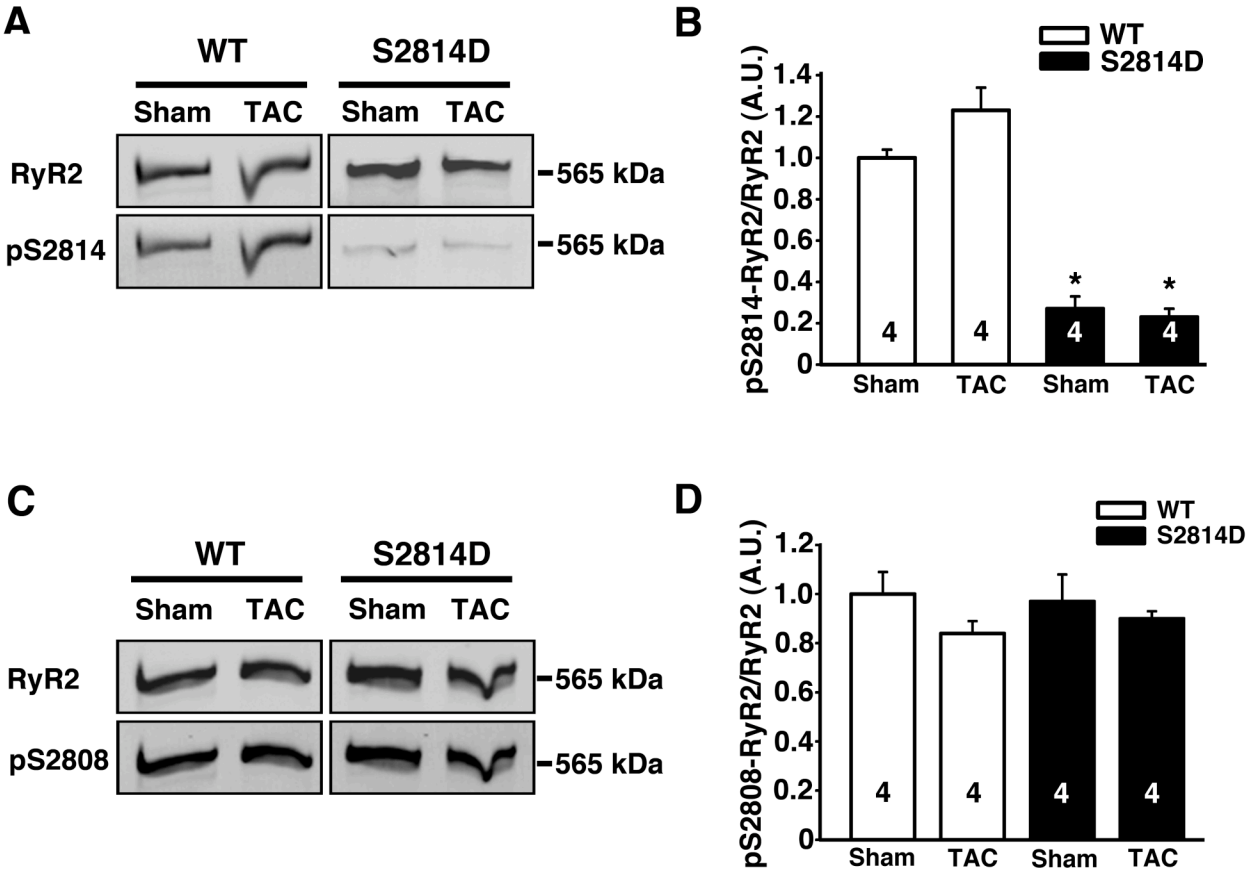
A
WT
S2814D
Sham
TAC
Sham
TAC
RyR2
pS2814
565 kDa
565 kDa
B
WT
S2814D
pS2814-RyR2/RyR2 (A.U.)
1.4
1.2
1.0
0.8
0.6
0.4
0.2
0
4
4
4
4
*
*
Sham
TAC
Sham
TAC
C
WT
S2814D
Sham
TAC
Sham
TAC
RyR2
pS2808
565 kDa
565 kDa
D
WT
S2814D
pS2808-RyR2/RyR2 (A.U.)
1.2
1.0
0.8
0.6
0.4
0.2
0
4
4
4
4
Sham
TAC
Sham
TAC

Supplemental References

1. Chelu MG, Sarma S, Sood S, Wang S, van Oort RJ, Skapura DG, Li N, Santonastasi M, Muller FU, Schmitz W, Schotten U, Anderson ME, Valderrabano M, Dobrev D, Wehrens XH. Calmodulin kinase II-mediated sarcoplasmic reticulum Ca2+ leak promotes atrial fibrillation in mice. *J Clin Invest.* 2009;119:1940-1951.
2. Zhang R, Khoo MS, Wu Y, Yang Y, Grueter CE, Ni G, Price EE, Jr., Thiel W, Guatimosim S, Song LS, Madu EC, Shah AN, Vishnivetskaya TA, Atkinson JB, Gurevich VV, Salama G, Lederer WJ, Colbran RJ, Anderson ME. Calmodulin kinase II inhibition protects against structural heart disease. *Nat Med.* 2005;11:409-417.
3. Sood S, Chelu MG, van Oort RJ, Skapura D, Santonastasi M, Dobrev D, Wehrens XH. Intracellular calcium leak due to FKBP12.6 deficiency in mice facilitates the inducibility of atrial fibrillation. *Heart Rhythm.* 2008;5:1047-1054.
4. Guo T, Zhang T, Mestril R, Bers DM. Ca2+/Calmodulin-dependent protein kinase II phosphorylation of ryanodine receptor does affect calcium sparks in mouse ventricular myocytes. *Circ Res.* 2006;99:398-406.
5. Pereira L, Metrich M, Fernandez-Velasco M, Lucas A, Leroy J, Perrier R, Morel E, Fischmeister R, Richard S, Benitah JP, Lezoualc'h F, Gomez AM. The cAMP binding protein Epac modulates Ca2+ sparks by a Ca2+/calmodulin kinase signalling pathway in rat cardiac myocytes. *J Physiol.* 2007;583:685-694.